Taylor & Francis
Taylor & Francis Group

Experimental Heat Transfer

A Journal of Thermal Energy Generation, Transport, Storage, and Conversion

ISSN: 0891-6152 (Print) 1521-0480 (Online) Journal homepage: www.tandfonline.com/journals/ueht20

Experimental investigation of the heat transfer characteristics of a synthetic annular jet impingement on a flat surface

Unal Akdag, Selma Akcay, Necati Un & Merdin Danismaz

To cite this article: Unal Akdag, Selma Akcay, Necati Un & Merdin Danismaz (2025) Experimental investigation of the heat transfer characteristics of a synthetic annular jet impingement on a flat surface, Experimental Heat Transfer, 38:5, 465-484, DOI: 10.1080/08916152.2024.2356165

To link to this article: https://doi.org/10.1080/08916152.2024.2356165

EXPERIMENTAL HEAT TRANSFER
2025, VOL. 38, NO. 5, 465–484
https://doi.org/10.1080/08916152.2024.2356165

Taylor & Francis
Taylor & Francis Group

Experimental investigation of the heat transfer characteristics of a synthetic annular jet impingement on a flat surface

Unal Akdag[a], Selma Akcay[b], Necati Un[a], and Merdin Danismaz[c]

[a]Department of Mechanical Engineering, Engineering Faculty, Aksaray University, Aksaray, Turkey; [b]Department of Mechanical Engineering, Engineering Faculty, Cankiri Karatekin University, Cankiri, Turkey; [c]Department of Mechanical Engineering, Engineering and Architecture Faculty, Kırşehir Ahi Evran University, Kirsehir, Turkey

ABSTRACT

Annular impinging jets create a more uniform flow on the impact surface compared to circular impinging jets, allowing the surface to cool better. Additionally, periodic flow oscillations significantly increase heat transfer by reducing the thermal resistance on the surface. Therefore, this study experimentally investigated the heat transfer characteristics of a synthetic annular jet impinging on a flat surface with constant heat flux. In the experiments, the jet-target surface distance (H/D), jet Reynolds number (Re_j), oscillation amplitude (A_o), and Womersley number (Wo) were changed. In contrast, the Prandtl number (Pr) and other geometric parameters were kept constant. The effects of these parameters on heat transfer were analyzed and the results were compared with continuous circular and annular impinging jets. Local temperature values on the target surface were obtained for different parameters and heat transfer from the surface was calculated. Experimental results showed that heat transfer increased with decreasing H/D ratio for all jet types. The highest heat transfer on the surface was achieved in synthetic jet flow. Heat transfer increased as the oscillation amplitude decreased. It was observed that there is a specific value for the Womersley number (Wo = 94) and that the heat transfer decreases after this value. For $Re = 50000$ and H/D = 2, the annular jet provided 27% higher heat transfer than the circular jet. In synthetic jet flow, heat transfer at H/D = 2 was improved by 21% compared to H/D = 8 for $Re = 6000$, $A_o = 1.87$ and $Wo = 163$.

ARTICLE HISTORY
Received 28 March 2024
Accepted 10 May 2024

KEYWORDS
Annular jet; synthetic impingement jet; flat target surface; heat transfer enhancement

Introduction

Different methods that increase heat transfer in engineering applications such as heating, cooling and drying are being investigated in the industry. In these researches, it is seen that impinging jets are widely used to increase the heat transfer rate [1, 2]. Impinging jet flow is achieved by passing the fluid through a blower such as a nozzle or duct and impinging the target surface at high speed. The impinging jet mechanism is based on increasing heat transfer by removing or thinning the boundary layer formed on the target surface. Impinging jets are used in the drying, heating, and cooling processes of various applications such as cooling of gas turbine blades and electronic circuit elements, food processing, annealing of metals, textile, paper, glass, and chemical industries [3]. The flow and heat transfer properties of impinging jets vary depending on many parameters such as jet exit geometry, jet velocity, jet temperature, distance between the jet and the plate, flow regime of the jet, geometry, and temperature of the target surface [4–6]. Dhruw et al. [7] examined the effects of inclined circular jets impinging a flat target surface on heat transfer, while Talapati and Katti [8] investigated

CONTACT Unal Akdag uakdag@aksaray.edu.tr Department of Mechanical Engineering, Engineering Faculty, Aksaray University, Aksaray, Turkey

the effects of multiple circular jets on a semicircular concave target surface. The effects of impinging jets on heat transfer have been studied for a long time by experimental and numerical studies [9]. Some of these studies focused on jet exit geometry (circular, annular, elliptical, triangular, polygonal, and swirl type) [5, 10]. The results of the study reported that the coaxial annular jet is more effective than the circular jet in heat transfer [11, 12]. For this reason, studies have focused on annular jet flows.

Çelik and Turgut [13], analyzed many jet parameters affecting heat transfer (such as Reynolds number, distance between nozzle and target surface, jet type, and surface roughness) with the Taguchi method in their experimental studies. In their study, they presented a comprehensive study considering Reynolds numbers in the range of $20{,}000 \leq Re \leq 40{,}000$ and four different nozzle-target surface distances (H/D: 2,6,8 and 10). They reported that the Reynolds number has a significant effect on surface cooling, heat transfer on a rough impact surface is higher than on a smooth surface, and the Nusselt number decreases as the H/D distance increases. Finally, the use of a coaxial annular jet provides better heat transfer than the use of a single circular jet. Afroz and Sharif [14] numerically examined the effects of a continuous annular impinging jet on an isothermally heated flat surface for different Reynolds numbers ($5{,}000 \leq Re \leq 35{,}000$) and jet-target surface distances ($0.5 \leq H/D \leq 4$). As a result of the study, it was reported that the Nusselt number increased as the H/D distance decreased. They stated that the annular impinging jet provided 15% more heat transfer than the circular jet. In an experimental study, Terekhov et al. [15] investigated the annular impinging jet flow for $12{,}000 \leq Re \leq 36000$ and $2 \leq H/D \leq 6$ and found that in the case of H/D = 2, the annular jet improved the heat transfer by 70% compared to the circular jet. Fenot et al. [16] experimentally investigated the heat transfer characteristics of annular impinging jets according to the D_{inner}/D ratio and found that the heat transfer on the surface increased as the ratio of inner diameter to outer diameter increased. They found that the Nusselt numbers obtained when the D_{inner}/D ratios were 0.35, 0.7, and 0.85 were Nu = 210, Nu = 290, Nu = 430, respectively. Dutta and Chattopadhyay [17], examined the effects of continuously impinging annular jets on heat transfer for different Reynolds numbers ($10{,}000 \leq Re \leq 50{,}000$) for H/D = 2 and reported that the Nusselt number increases with increasing Reynolds number. Dutta et al. [18] numerically examined the effects of annular impinging jet arrays on a moving surface on flow and heat transfer and showed that thermal performance is strongly affected by surface movement and that heat transfer is improved at high surface velocities. Some studies have investigated the effects of jet numbers on heat transfer [19, 20]. Barbosa et al. [19] presented a review study investigating the effects of multiple impinging air jets on convective heat transfer and discussed the advantages and disadvantages of numerical models used in modeling impinging jets. They also presented the proposed correlations for the Nusselt number, which characterizes the heat transfer in single and multiple impinging air jets. Tu et al. [21] numerically examined the flow and heat transfer by using a sweep jet actuator to cool the blades of high-temperature gas turbines. They analyzed the effects of circular jet and sweeping jet for different H/D ratios and reported that the sweeping jet caused a more uniform and regular heat transfer at the leading edge of the wing in the case of H/D = 5.

The above studies reported that heat transfer can be improved if appropriate jet parameters are used in a continuous impinging jet. However, in cases requiring higher heat transfer, such as cooling turbine blades and electronic components, methods that provide effective cooling are needed [9]. Among these methods, oscillatory flows have a significant potential because they provide a high heat transfer rate [22, 23]. Synthetic jets, a method in which oscillatory flows are used, have zero net mass flux and the working principle and design of these jets are quite simple. Synthetic jets periodically absorb some fluid from the main flow and blow it back onto the target surface, creating time-dependent effects in the flow and giving the flow a non-linear behavior. It is known that the unsteady flow structure is more effective than the steady flow structure. Synthetic jets have significant advantages and attract the attention of many researchers because they create an unstable flow structure, do not require an additional fluid source, and oscillation parameters can be easily controlled [1, 24]. For this reason, periodic impinging jets such as synthetic jets have become the focus of research in recent years. In synthetic jets, oscillatory motion is generally provided by acoustic actuators such as speakers, piezo-electric diaphragms, plasma synthetic jet actuators (spark spray), or piston-cylinder

mechanisms [24–26]. Therefore, these mechanisms are used to determine the range of oscillation amplitude and frequency. The amplitude and frequency of oscillation are among the important parameters affecting heat transfer in periodic flows. In impinging jet applications, examining the oscillation parameters along with the jet parameters expands the studies on this subject.

Maghrabie [1] presented an exhaustive review study, taking into account the geometric and operating parameters of impinging jets used in various engineering applications. The study reviewed different jet impingement techniques, including passive self-propelled jets, active-propelled jets such as synthetic jets, and hybrid-propelled jets. Travnicek and Tesar [27] experimentally examined the synthetic annular impinging jet flow with a D_{in}/D_{out} ratio of 0.95 at a constant jet velocity and different frequency values, using an acoustic stimulus for oscillatory motion. Sarma et al. [28] experimentally examined the flow and heat transfer characteristics on the target surface using a synthetic jet actuator at different synthetic amplitudes, Strouhal numbers (St), and jet-target surface ratios for $3000 \leq Re \leq 6000$. It was observed that the synthetic jet parameters have an impact on the formation of dominant regions on the target surface. It was also found that when the jet-target surface ratio is low, the heat transfer is lower at high St compared to low St. Trávníček et al. [29] experimentally investigated the heat transfer characteristics on the impact surface of 12 synthetic annular jets with $D_{in} = 74$ mm and $D_{out} = 84$ mm at different nozzle-target surface distances and a constant air jet velocity ($u_{jet} = 5$ m/s). In their experiments, they provided periodic flow components using an electric actuator. In an experimental study, Mangate and Chaudhari [30] examined the effects of synthetic impinging jets in the 100–250 Hz oscillation frequency range on the cooling of electronic devices for circular and oval nozzles with the same hydraulic diameter. As a result of the study, they found that oval nozzles provide higher heat transfer than circular nozzles. In an experimental study, Donovan and Murray [31] investigated the periodic impinging jet flow at different jet-target surface distances ($H/D = 0.5–2.0$) and used an acoustic actuator to control the oscillation frequency. Krishan et al. [32] presented a review study examining the effects of synthetic impinging jets on heat transfer for different jet parameters.

Arshad et al. [33] carried out an important review study investigating synthetic jet actuators on heat transfer. Another review study that includes impinging jet applications in heat transfer improvement was conducted by Plant et al. [9]. As a result of their study, they reported that the distance between the jet and the target surface, the type of fluid, and nonstandard jets such as synthetic jets have significant effects on heat transfer. In a numerical study, Tan et al. [34] compared the heat transfer of continuous and synthetic jets with different jet geometries (round, square, rectangular) and showed that continuous jets exhibited a higher heat transfer coefficient around the stagnation point, while synthetic jets provided a more uniform heat transfer on the surface. They also reported that as the distance between the jet and the target surface increases, synthetic jets provide stronger and wider effective heat transfer than continuous jets. They found that the rectangular jet provides higher heat transfer at the stagnation point compared to other jet geometries in synthetic jet flows. Panda et al. [24] examined the temperature measurements of a synthetic jet actuator created using piezo-electric diaphragms. They analyzed the jet flow passing through inner and annular holes with equal hydraulic diameters ($d_h = 3$ mm) for $Re = 1100$. They found that excitation voltage rather than oscillation frequency was more effective on the strength and spread of the synthetic jet. Deng et al. [35] experimentally compared the effects of dual synthetic impinging jets on surface cooling compared to single synthetic impinging jets. They reported that in both cases, maximum heat transfer was achieved when $H/D = 5.5$, and 11.4% higher heat transfer was achieved in the double-impinging synthetic jet flow. Akdağ et al. [36] experimentally and numerically investigated the heat transfer characteristics of a pulsating impinging jet on a flat surface with constant heat flux. They analyzed the effects of changing pulsating amplitude and frequency at different jet-target surface distances (H/D: 2, 4, 6) for a constant flow rate. They reported that the effect of frequency on temperature change was low at low amplitudes and that heat transfer improved by approximately 30% with increasing amplitude and frequency at $H/D = 2$. Singh et al. [37] Experimentally examined the thermal behavior of synthetic jets

with different geometries (rectangular, isosceles, and equilateral triangle) in three different waveforms (square, triangular and sinusoidal). They reported that in the triangular waveform for all hole geometries achieved higher heat transfer. They also found that synthetic jets with rectangular geometry provide 32% and 16.5% higher heat transfer than jets with isosceles and equilateral triangular geometry, respectively. In another experimental study, Singh et al. [38] investigated the effects of synthetic impinging jets on heat transfer in different waveforms (square, triangular and sine) using single and multiple orifices for Re = 3525. They reported that multiple synthetic jets provide 30.6% higher heat transfer than single synthetic jets.

In previous studies, coaxial annular jets were mostly examined under continuous flow conditions, numerical methods were mostly used in the studies, a periodic oscillatory motion was mostly provided by mechanisms such as acoustic systems and diaphragms, the frequency and amplitude forming the jet parameters were examined in a limited range. In studies involving synthetic jets, it is seen that circular jets are mostly used. Therefore, in this study, the effects of coaxial annular synthetic jet on flow and heat transfer were experimentally examined for different oscillating parameters. Additionally, the study results were compared with continuous circular and continuous annular jet flows

Experimental study

In the experimental study, continuous impinging circular jets (CCJ), continuous impinging annular jets (CAJ), and synthetic annular impinging jets (SAJ) were examined for different parameters. The schematic view of the mechanism in which the experiments were carried out is given in Figure 1a, and its real view is given in Figure 1b.

The fluid used in the study is air. A high-pressure fan (1) was used to create the jet flow. The fluid coming out of the fan is connected to the velocity meter (2) with a flexible hose and the velocity of the fluid is measured with a turbine-type velocity meter (Testo-435). The fluid adjusted to the tested velocity enters the distributor (3) through the flexible hose. The distributor has to supply a uniform

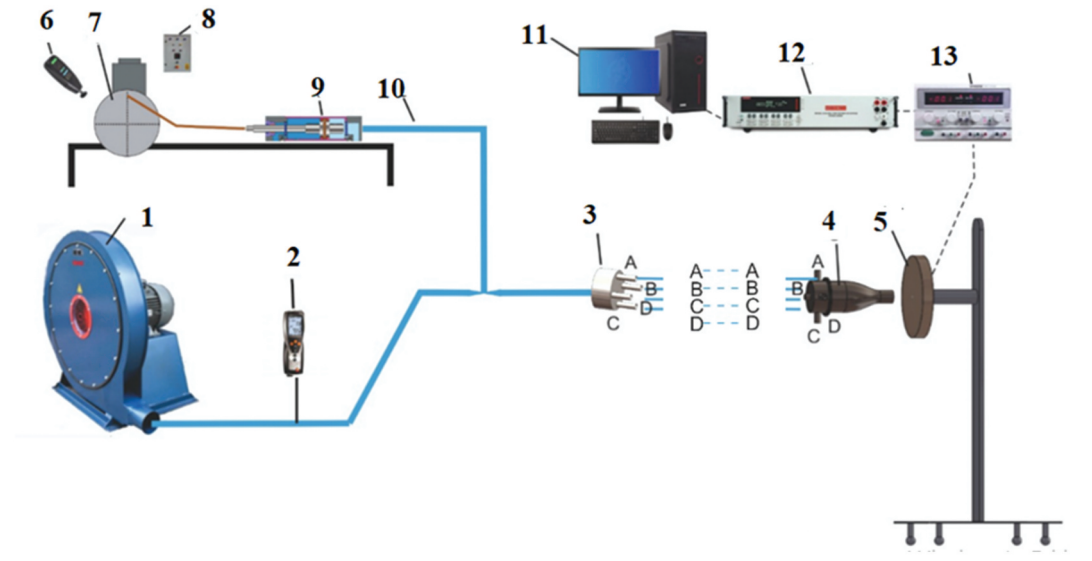

Figure 1a. Schematic view of the experimental setup.
(1. High pressure fan, 2. Velocity meter, 3.Distributor, 4. Nozzle 5. Target surface, 6. Digital tachometer, 7. Flywheel, 8. DC motor and control unit, 9. Piston-cylinder mechanism, 10. Blowpipe, 11. CPU, 12. Data acquisition system, 13. Power supply)

Figure 1b. Real view of the experimental setup.

and adequate flow rate of fluid to the nozzle (9). The fluid collected in the distributor enters the mixing chamber of the nozzle through 4 flexible hose connections.

The geometry of the nozzle was designed to create circular and annular jets. The jet blower was drawn in the Solidworks modeling program, manufactured using 1.75 mm diameter PLA filament on a 3D printer, and then assembled. During the assembly phase, an air inlet was provided to the 58 mm length mixing chamber through four separate flexible hose connections that do not deform. There is a honeycomb-shaped flow straighteners after the mixing

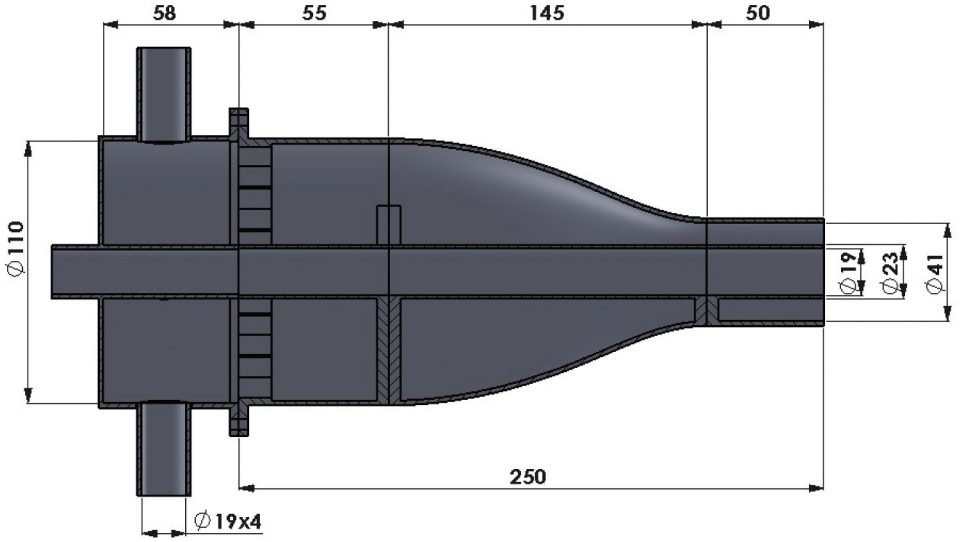

Figure 2. Geometry of the nozzle (dimensions in mm).

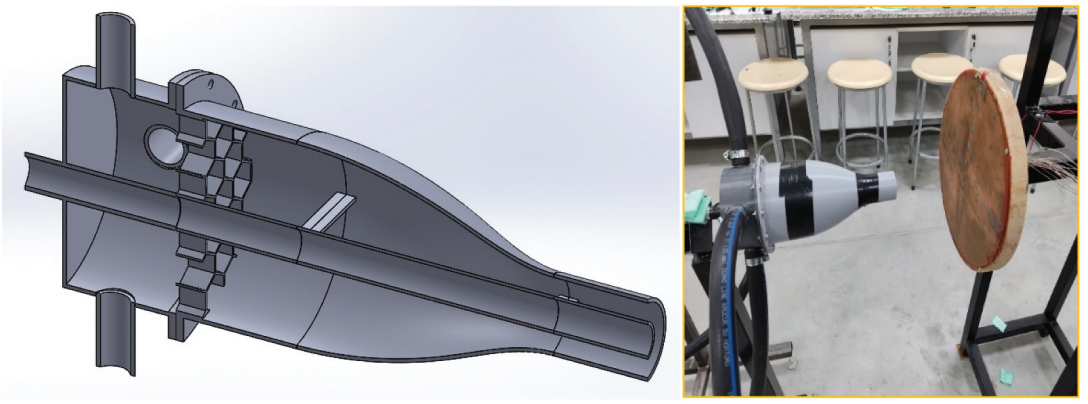

a b

Figure 3. a) Cross-sectional view of the nozzle, b) Nozzle and target surface view.

chamber. Thus, it is aimed that the fluid passing through the flow conditioner at the nozzle entrance enters the annular section uniformly and homogeneously. Figure 2 shows the shape and geometric properties of the nozzle in detail. The diameter of the circular nozzle is 19 mm. The outer diameter of the coaxial annular nozzle is $D_{out} = 41$ mm. The total nozzle length is 250 mm. Figure 3 indicates the cross-sectional view of the nozzle (Figure 3a) and the final image of the jet and target surface (Figure 3b). Nozzle dimensions were determined based on target surface size and literature studies [36].

The synthetic impinging jet mechanism is created to give synthetic jet flow to the mass flux coming from the high-pressure fan. This mechanism consists of a piston-cylinder (9), a flywheel (7), a DC motor (2.4 KW) that moves the flywheel, and a speed adjustment unit (8) that controls the speed setting of the DC motor. The amplitude of the oscillation can be adjusted through the holes drilled on the flywheel, and the frequency can be adjusted by changing the engine speed. The speed of the DC motor can be read via a digital tachometer (6). The piston-cylinder mechanism is connected to the mixing chamber of the nozzle (4) with a flexible hose. The fluid coming from the high-pressure fan oscillates by the synthetic jet mechanism, allowing the fluid to impingement the target surface (5).

The target surface consists of a circular flat copper plate with a diameter of 30 cm and a thickness of 2 mm. Temperature measurements are conducted for the determined parameters on the target surface. Temperature measurements are carried out with the help of a total of 25 thermocouples placed on the surface. Two thermocouples are used to determine the ambient and jet temperatures. Thermocouples are placed on the surface at certain distances along the x and y axes from the center of the plate. The positions of the thermocouples on the plate surface are shown in Figure 4a. Thermocouples were placed in the grooves cut on the copper plate, and then the grooves were filled with solder to ensure that the thermocouples were fixed to the surface. The target surface was sanded to obtain a smooth surface. A Kapton heater and 20 mm rock wool insulation material were placed behind the copper plate (Figure 4b). The Kapton heater is connected to the power supply (13) to obtain constant heat flux. The front surface of the copper plate was left open facing the jet, and the other surfaces were embedded in a specially prepared wooden frame. With the rock wool insulation material, the heat is transferred completely from the front surface. For this reason, heat losses from other aspects of the plate are neglected. The structure of the target surface is given in Figure 4b. Instant temperature values read from thermocouples on the copper plate surface were transferred to the computer (11) with a data acquisition system (12).

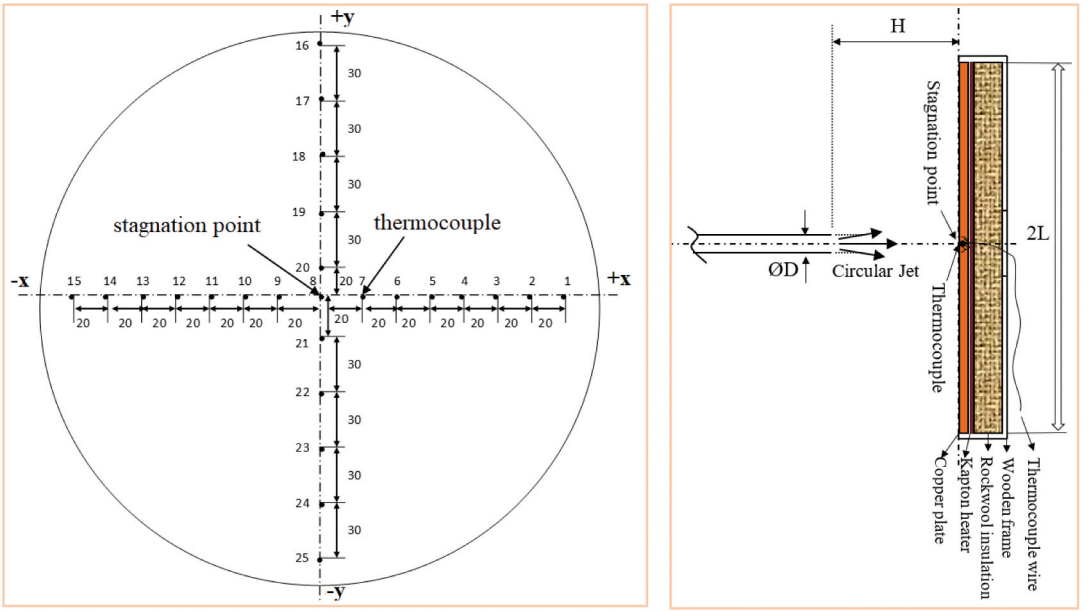

Figure 4. a) Positions of thermocouples placed on the target surface, b) Target surface structure.

Data reduction

In this study, the effects of continuous circular jet (CCJ), continuous annular jet (CAJ), and synthetic annular jet (SAJ) were investigated in order to cool the target surface with constant heat flux. The jet parameters used in the study are explained in this section.

Continuous jet Reynolds number (Re_j) was calculated with Eq. 1:

$$Re_j = \frac{U_j D_h}{\upsilon} \tag{1}$$

where D_h indicates the hydraulic diameter of the jet. Circular jets and annular jets have the same hydraulic diameter. U_j is the jet exit velocity and is measured with a Testo 435 velocity meter.

Synthetic jet Reynolds number (Re_j) was calculated with Eq. 2:

$$Re_{syn,j} = \frac{u_{sj} D_h}{\upsilon} \tag{2}$$

Synthetic jet velocity ($U_{syn,j}$) theoretically is given by Eq. 3:

$$U_{syn,j} = u_{sj}[1 + A_o sin(\omega t)] \tag{3}$$

where A_o indicates the dimesionless amplitude, ω is angular velocity (rad/s), t is time (s).

Dimensionless distance between the jet and the target surface (B) is given in Eq. 4:

$$B = H/D_h \tag{4}$$

where H indicates the distance between the jet exit and the target surface.

Dimensionless amplitude (A_o) is found with Eq. 5:

$$A_o = \frac{x_m}{L} \tag{5}$$

where, x_m is the amplitude of the piston and L is the characteristic length and the radius of the target surface.

Womersley number (Wo) is used as the dimensionless frequency and Eq. 6 is calculated:

$$Wo = \sqrt{\omega/\upsilon} \tag{6}$$

Here, ω (rad/s) represents the angular velocity and υ (m^2/s) represents the kinematic viscosity. Prandtl number (Pr) is calculated with Eq. 7.

$$Pr = \frac{\upsilon}{\alpha} \tag{7}$$

$$\alpha = \frac{k}{\rho C_p} \tag{8}$$

Here, α expresses the heat dissipation coefficient, C_p the specific heat, k the heat conduction coefficient, and ρ the density of the fluid. Air was used as the fluid in the experiments, and it was assumed that the thermophysical properties of the fluid did not change.

Experimental procedure

In the experiments, three different jet flows were examined: CCJ, CAJ, and SAJ. For CCJ and CAJ, the effects of 4 different jet-target surface distances ($2 \le H/D \le 8$) and different Reynolds numbers ($6000 \le Re \le 50000$) were investigated. For SAJ, The effects of 4 different oscillation amplitudes (A_o: 0.47, 0.93, 1.4, 1.87), 6 different oscillation frequencies (Wo: 67, 94, 116, 135, 150, 163), 4 different jet-target surface distance ($2 \le H/D \le 8$) and different Reynolds numbers ($6000 \le Re \le 25000$) were examined.

First of all, the experiments were carried out for continuous impinging jet flow where only the high-pressure fan was active (steady flow regime). Continuous impinging jet flow involves experiments in which the synthetic jet mechanism is closed and only the fan is active. For CCJ flow, the fan is activated after the distance (H) between the jet and the target surface is determined. With the help of the velocity meter, the flow rate is adjusted to the tested value. The heater is activated to heat the target surface. Thus, a constant heat flux is provided to the copper plate and the plate begins to heat up. A certain period is waiting for the system to become a regime. It is determined from temperature measurements that the system has entered a regime state. If the temperature values read from each of the thermocouples placed on the copper plate do not change, it is understood that the system has entered a regime state and the instantaneous temperature values are recorded on the computer through the data acquisition system. For continuous circular impinging jet flow, the experiments are repeated by changing the distance between the nozzle and the target surface and the Reynolds numbers. Then, the heat transfer occurring on the plate surface is calculated with the help of the temperature data recorded for the continuously impinging jet flow. In CAJ flow, the air inlet of the 19 mm diameter circular channel passing through the center of the nozzle is closed and an annular jet is formed. The other experimental procedure for CAJ flow is as described above. Then, the temperature values obtained from the CCJ and CAJ experiments are compared. Additionally, the experimental results were compared with the results obtained from previous studies.

SAJ flow includes experiments performed when the synthetic jet mechanism is active along with the high-pressure fan. In synthetic jet flow, the fan is active and the velocity of the fluid coming from the fan to the nozzle is adjusted to the tested value with the velocity meter. To create a synthetic jet, first, the amplitude of the oscillation is adjusted to the tested position on the flywheel. The flywheel is driven by activating the 2.4 kW DC motor. Then, the oscillation frequency is adjusted to the tested value with the help of the motor speed control unit. Finally, the pneumatic piston-cylinder mechanism is activated and thus, the fluid coming from the fan is

provided with an oscillatory movement at the specified amplitude and frequency. All synthetic impinging jet experiments were carried out for coaxial annular jets. In SAJ experiments, the fluid impinges on the target surface with constant heat flux, and the system is expected to move away from transient conditions and become a regime. When the system becomes a regime, the instantaneous temperature values read from each thermocouple on the target surface are transferred to the computer via the data acquisition system. For SAJ, experiments are repeated by changing the distance between the nozzle and the target surface, Reynolds number, oscillation amplitude, and oscillation frequency. Then, the heat transfer occurring on the plate surface is calculated with the help of the temperatures recorded for the SAJ.

Validation of the experiment results

In their previous experimental studies, the authors compared the heat transfer obtained over a flat surface in CCJ flow for H/D = 2 and Re = 15000 values with the numerical study results of Xu et al. [23] and with the experimental and numerical study results of Rakhsha et al. [39]. The comparison of the results obtained is explained in detail in the authors' previous study [36]. In this study, similar geometry and flow type were used for the continuous circular impinging jet and it was considered sufficient and appropriate to verify the solutions. Figure 5 indicates validation of the present study with previous studies [23, 36, 39]

Determination of the plate surface temperature

In this section, the temperature values obtained on the target surface for CCJ, CAJ, and SAJ flows are presented. For temperature measurements in continuous jet flow, temperature values taken from each thermocouple on the target surface were transferred to the computer through a data acquisition system. The average temperature of the target surface is calculated by the arithmetic average of the temperature values taken from each thermocouple. In synthetic jet flow, temperature values change instantaneously due to periodic flow. For this reason, instantaneous temperature values taken from each thermocouple on the target surface are recorded on the computer with the data acquisition system. Then, the average temperatures of these points are calculated by taking the time average of the instantaneous temperature values taken from each thermocouple. The local average temperature values of each thermocouple on the target surface were calculated with Eq. 9, since the time intervals (Δt) were equal [36].

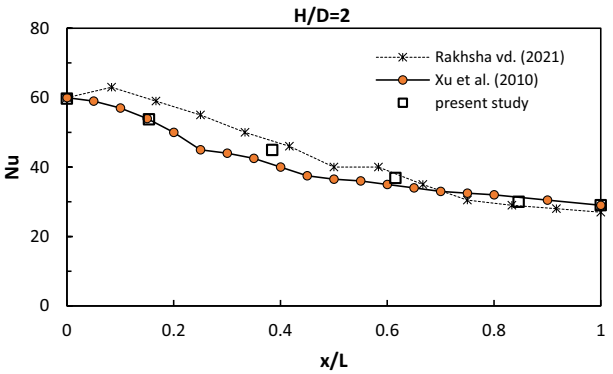

Figure 5. Validation of the present study with previous studies [23, 33].

$$\bar{T}w, y = \frac{1}{N\Delta t}\sum_{i=1}^{N} Tw, i(y,t)\Delta t \tag{9}$$

Here N is the total number of data, Δt is the time interval and T_w is the instantaneous surface temperature. The average temperature of the target surface ($\bar{T}_w$) is obtained by Eq. 10.

$$\bar{T}_w = \frac{T_{w,1} + T_{w,2} + T_{w,3} + \ldots\ldots\ldots + T_{w,11}}{11} \tag{10}$$

Constant heat flux to the target surface is provided by transferring the electrical power (θ_{el}) applied by the power source to the Kapton heater (Eq. 11). A constant heat flux of q" = 1200 W/m^2 is applied to the plate surface by the electric current (I = 2.72 A) and electric voltage (V = 31.2 V) applied to the Kapton heater by the power source (Eq. 12).

$$\theta_{el} = I.V \tag{11}$$

$$\theta_{heat} = \frac{\theta_{el}}{A_{plate}} = \frac{I.V}{\pi L^2} \tag{12}$$

Experiments for CCJ and CAJ flows were carried out at 4 different jet-target surface distances (H/D: 2, 4, 6, 8) and Reynolds numbers in the range of 6000≤Re ≤ 50000. The variation of the surface temperatures along the plate for different H/D and Reynolds numbers in CCJ flow is shown in Figure 6. It was observed that the surface temperatures decreased with increasing Reynolds number for all H/D ratios. In addition, the decrease in H/D ratios decreased the surface temperatures. Because the effect of the jet decreases as the distance between the jet and the target surface increases. Also, for all H/D and Reynolds numbers, it is seen that lower temperature values are obtained in the center of

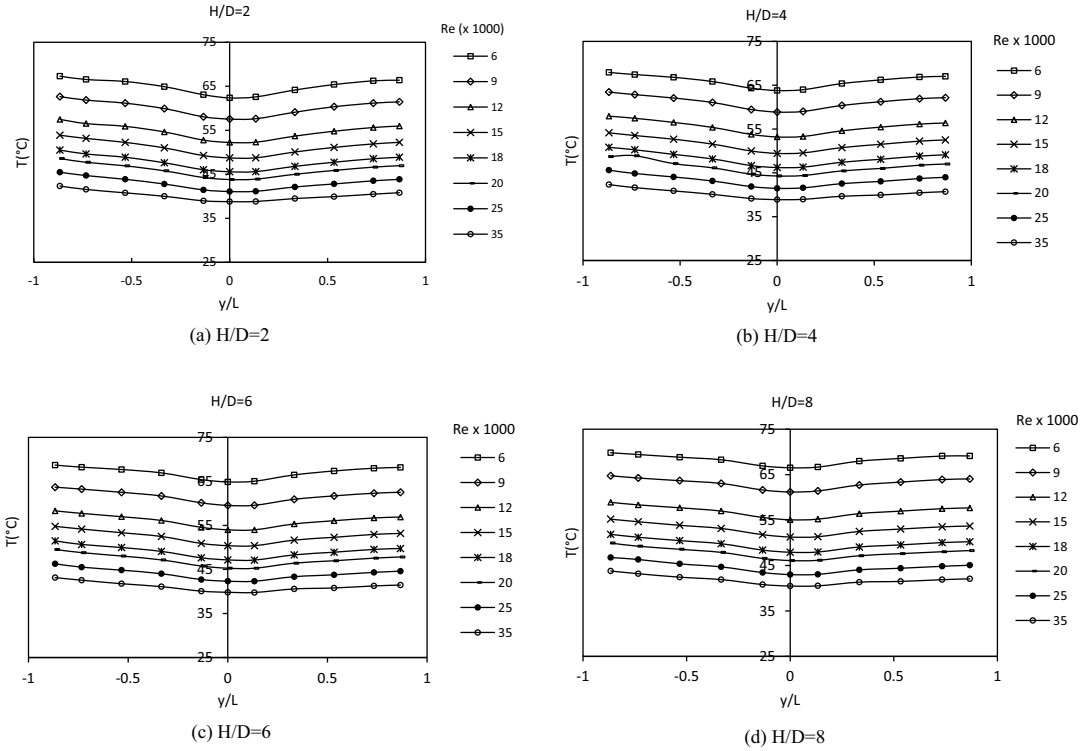

Figure 6. Variation of plate surface temperature in CCJ flow for different H/D and Re, (a) H/D=2, (b) H/D=4, (c) H/D=6, (d) H/D=8.

the plate and surface temperatures increase as we move away from the center of the plate. This is because the circular jet is more effective at the stagnation point on the target surface, and the effects of the jet decrease in the wall jet region. Since the target surface is circular, it has been observed that the temperature distribution in both directions from the stagnation point, which is the center of the plate, to the outside of the plate (along the -y and +y axis) is symmetrical. It has been observed that as the y/L ratio increases, the surface temperatures measured by thermocouples on the target surface also increase.

Figure 7 shows the variation of surface temperatures along the plate for different H/D ratios in CAJ flow and Reynolds numbers in the range of $6000 \leq Re \leq 50000$. It has been observed that surface temperatures decrease with increasing Reynolds number for all H/D ratios, as in CCJ flow. The decrease in the distance between the jet and the target surface caused the surface temperatures to decrease significantly. It has been observed that the difference between surface temperatures decreases after a certain Reynolds number ($Re \geq 15000$) at all H/D ratios. In CAJ, surface temperatures at the stagnation point were found to be higher than in the circular jet. This is because the jet does not directly hit the stagnation point due to the geometry of the coaxial annulus. At a constant Reynolds number, the temperatures obtained along the plate in the annular jet are more linear than in the circular jet. This shows that the annular jet is less active in the stagnation region and more effective in the wall jet region. Additionally, it was observed that the surface temperatures in the annular jet were lower than in the circular jet for the same parameters. Previous studies also support this result [13, 14]. The temperature distribution is symmetrical in both directions from the center of the target surface toward the tip of the plate. It is been observed that surface temperatures increase as the y/L ratio increases at low Reynolds numbers ($Re \leq 15000$). At medium and high Reynolds numbers ($Re \geq 18000$), it is observed that the surface temperatures along the plate approached parallelism. Since the annular jet impinges around the stagnation point, the temperature is lowest at distances close to the stagnation point, as expected. Temperatures increase distance from the target surface.

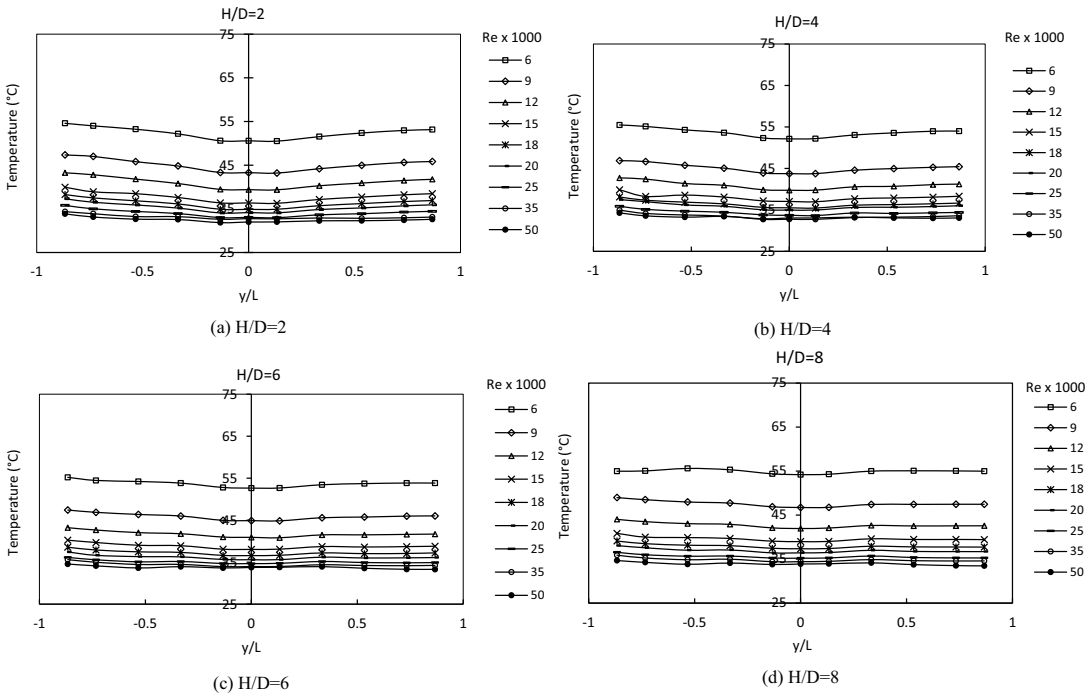

Figure 7. Variation of plate surface temperature in CAJ flow for different H/D and Re, a- H/D = 2, b- H/D = 4, c- H/D = 6, d- H/D = 8.

Table 1. Experimental parameters for synthetic annular jet.

Re	H/D	A_o	Wo
6000	2, 4, 6, 8	0.47, 0.93, 1.4, 1.87	67, 94, 116, 135, 150, 163
15000	2, 4, 6, 8	0.47, 0.93, 1.4, 1.87	67, 94, 116, 135, 150, 163
25000	2, 4, 6, 8	0.47, 0.93, 1.4, 1.87	67, 94, 116, 135, 150, 163

In the experimental study, the parameters used for SAJ flow are given in Table 1. For SAJ, since the main flow velocity from the fan suppresses the synthetic jet parameters at high Reynolds numbers, the experiments were carried out at low and middle Reynolds numbers (Re: 6000, 15000, 25000) and the results of the surface temperatures obtained from these experiments are presented.

In SAJ flow, the change of target surface temperatures for different oscillation amplitude (A_o) and oscillation frequency (Wo) in the case of Re = 6000 and H/D = 2 is given in Figure 8. It appears that synthetic jet parameters substantially affect plate surface temperatures. With increasing amplitude, surface temperatures significantly decreased. At low amplitudes (A_o = 0.47) the Womersley number has little effect on surface temperatures. As the oscillation amplitude increases, the effect of the Womersley number on surface temperatures is increased significantly. The difference between surface temperatures increases with increasing oscillation amplitude and frequency, for Re = 6000 and H/D = 2, the lowest surface temperatures on the plate surface were obtained at the parameters A_o = 1.87 and Wo = 163. The impact of the colder fluid coming out of the jet on the target surface, which is heated at high amplitude and high frequency, causes the velocity and thermal boundary layer formed on the plate to constantly deteriorate. This reduces thermal resistance and reduces surface temperatures.

In the experimental study, it was observed that the surface temperatures increased significantly as the H/D ratio increased in the annular jet flow. It has been observed that in the case of H/D = 2, the surface

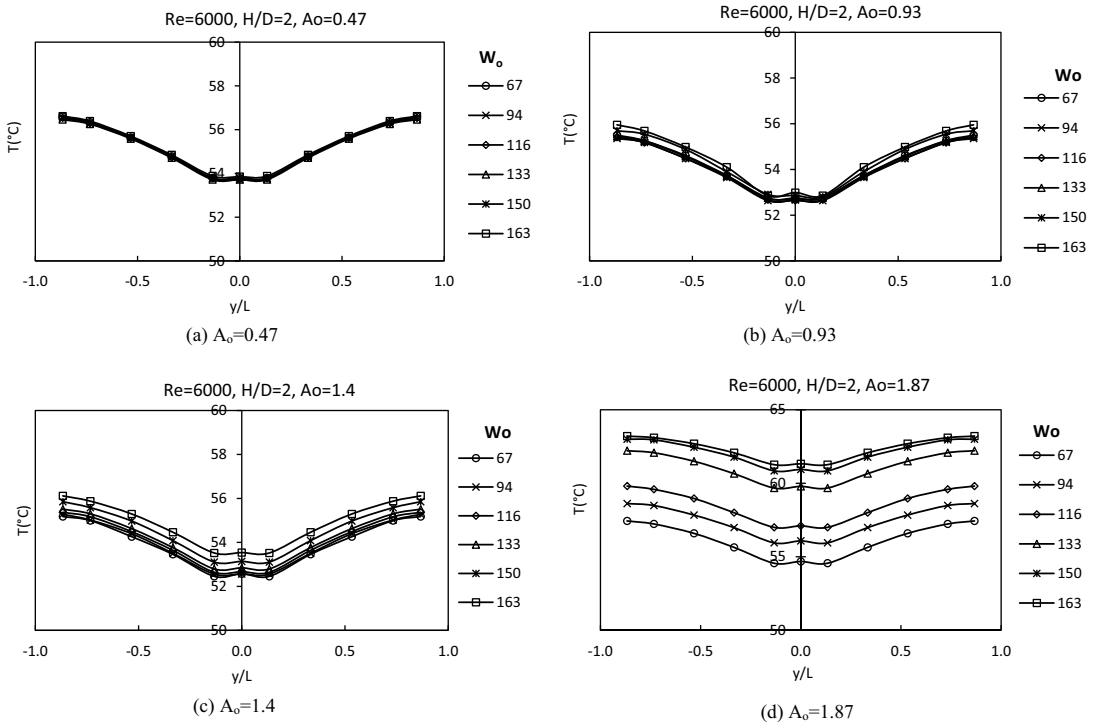

Figure 8. Variation of surface temperatures for different Ao and Wo in SAJ flow (Re = 6000 and H/D = 2), (a) Ao = 0.47, (b) Ao = 0.93, (c) Ao = 1.4, (d) Ao = 1.87.

temperatures are lower and the target surface is cooled better. It was determined that the surface temperatures were highest in the case of H/D = 8. The synthetic jet effect occurring with the piston-cylinder mechanism significantly affected the surface temperatures on the target surface, depending on the oscillation frequency and oscillation amplitude.

Heat transfer calculations

In the experiments, the heat transfer from the plate surface is determined by the Nusselt number (Nu). The local Nusselt number ($Nu_{y,t}$) and local heat transfer coefficient ($h_{y,t}$) are calculated with Eqs. 13 and 14, respectively.

$$Nu_{y,t} = \frac{h(y,t)L}{k} \tag{13}$$

$$h_{y,t} = \frac{q''}{T_{w(y,t)} - T_{j\infty}} \tag{14}$$

where L is the radius of the target surface and k is the heat conduction coefficient of the fluid. $T_w(y,t)$ and $T_{j\infty}$ are the instantaneous plate surface temperature and jet exit temperature, respectively. In the calculations, the characteristic length was taken as L. A periodic flow occurs in SAJ flow due to oscillation parameters. Time and location averaged values were taken into account in Nusselt number and heat transfer coefficient calculations. Time and location averaged heat transfer coefficient (h_m) and Nusselt number (Nu_m) are found with Eq. 15 and 16, respectively.

$$h_m = \frac{1}{\tau L}\int_0^{\tau}\int_0^{L} h(y,t)dydt \tag{15}$$

$$Nu_m = \frac{1}{\tau L}\int_0^{\tau}\int_0^{L} Nu_{y,t}dydt \tag{16}$$

As a result of the calculation of the above integrals, Eq. 17 was used for the average Nusselt number (Nu_{avg}).

$$Nu_{avg} = \frac{q''L}{k\left(\bar{T}w - T_{j\infty}\right)} \tag{17}$$

Where $\bar{T}_w$ is the average temperature of the target surface obtained by Eq. 10.

The heat transfer occurring on the target surface for CCJ and CAJ is given in Figure 9 for different H/D and Reynolds numbers. In CCJ flow, while the effect of H/D on heat transfer is not felt much at low Reynolds numbers (Re ≤ 15000), heat transfer increases with the decrease of H/D at medium and high Reynolds numbers (Re ≥ 18000). The highest heat transfer was obtained as Nu = 370.84 at Re = 50000 and H/D = 2 parameters (Figure 8a). It has been observed that the Nusselt number increases with the increase in Reynolds number and decrease in H/D in CAJ flow. The highest heat transfer was obtained as Nu = 507.9 at Re = 50000 and H/D = 2 parameters (Figure 8b). It is seen that CAJ provides higher heat transfer than CCJ. It has been determined that the annular jet provides approximately 27% higher heat transfer than the circular jet for the parameters Re = 50000 and H/D = 2.

The change of Nusselt number versus Womersley number for different Reynolds numbers at constant oscillation amplitude (A_o = 1.87) and constant jet-target surface distance (H/D = 2) in SAJ flow is presented in Figure 10. It was observed that the Nusselt number increased significantly with increasing jet velocity at a constant Wo value. It is been determined that at a constant jet velocity, there is a specific Wo value (Wo = 94), and heat transfer tends to decrease with increasing Wo values after

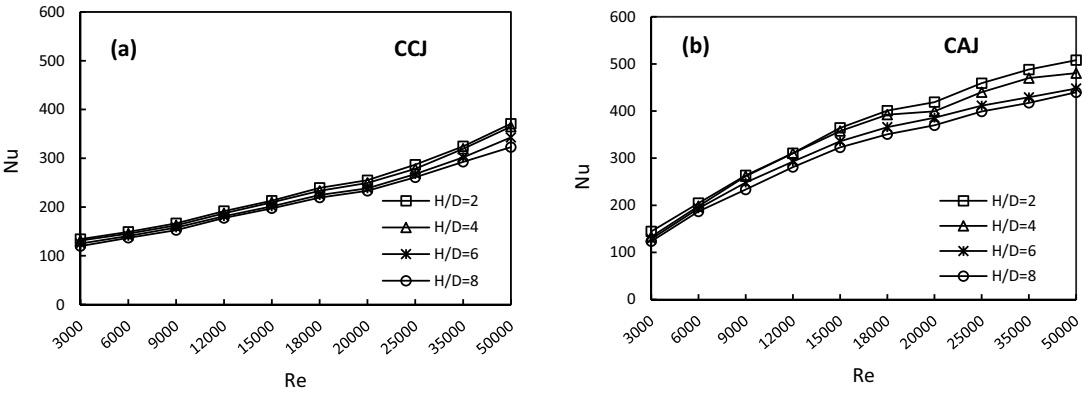

Figure 9. Nu versus Re with different H/D for continuous impinging jet, a) CCJ, b) CAJ.

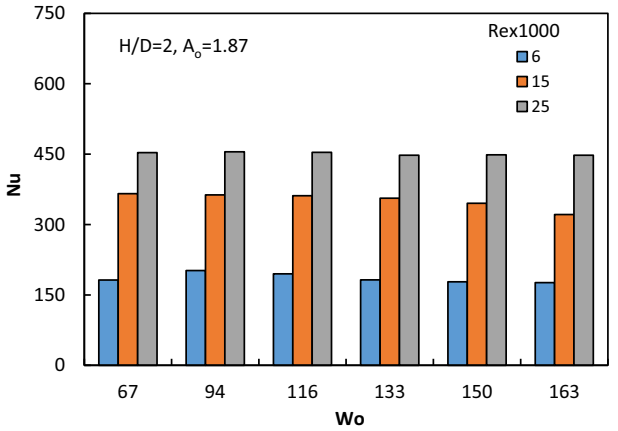

Figure 10. Nu versus Wo for different Re in SAJ flow (Ao = 1.87 and H/D = 2).

this value. This shows that increasing oscillation frequency brings the synthetic jet flow closer to steady flow conditions. Therefore, increasing the frequency of SAJ flow will cause the heat transfer to decrease. For constant values of $A_o = 1.87$ and H/D = 2, the best heat transfer was obtained as Nu = 455.11 at Re = 25000 and Wo = 94.

For SAJ flow, the variation of oscillation amplitude and frequency and Nusselt number for different jet-target surface distances at a constant Reynolds number (Re = 6000) is presented in Figure 11. It can be seen from the figures that heat transfer decreases with increasing H/D. At other H/D ratios except H/D = 2, the increase in oscillation amplitude and oscillation frequency caused the heat transfer on the target surface to decrease. Increasing the amplitude increases the withdrawal time of the air, ensuring that the surface remains warmer. This situation causes the heat transfer over the surface to decrease. At low amplitude, since the fluid hits the surface in shorter time intervals, it prevents the formation of a thermal boundary layer on the surface. Thus, thermal resistance decreases, and heat transfer increases. At H/D = 2, the Nusselt numbers were obtained close to each other for all Wo values at the oscillation amplitudes of $A_o = 0.93$ and $A_o = 1.4$, and it was observed that the obtained Nusselt numbers were higher than the other amplitudes. The lowest heat transfer occurred at $A_o = 1.87$. At low jet velocities, increasing the amplitude and frequency reduces the effect of the jet.

Nusselt numbers obtained at different H/D ratios for fixed parameters Re = 6000, $A_o = 1.87$, and Wo = 163 are compared in Figure 12a. It has been observed that heat transfer decreases as the distance

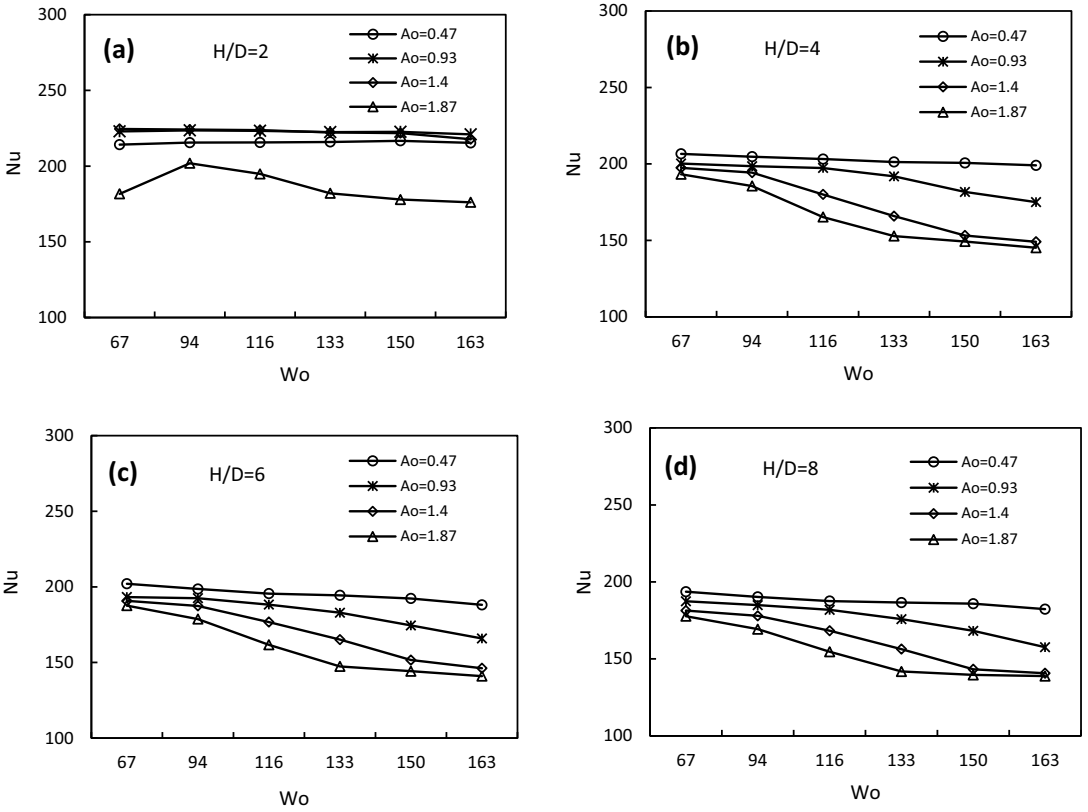

Figure 11. Nusselt number versus Wo at different amplitudes in SAJ flow (Re = 6000).

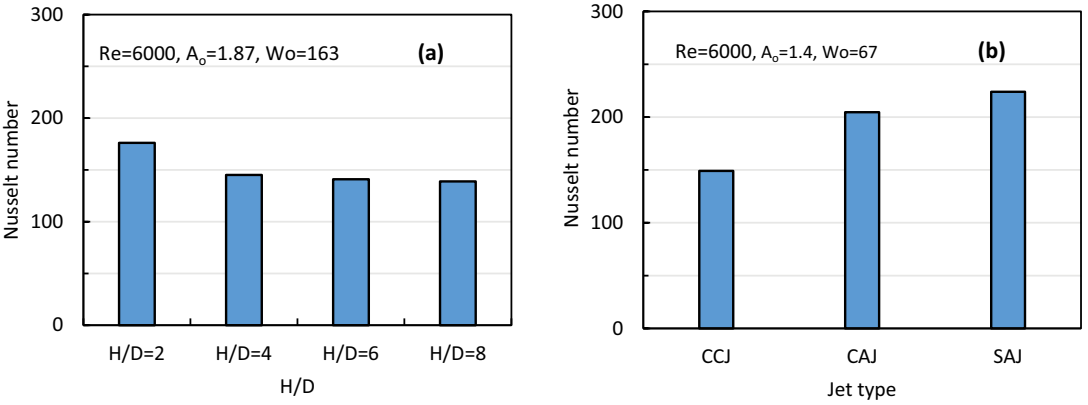

Figure 12. For constant Ao, Wo and Re in jet flows a) H/D versus Nu, b) Jet type versus Nu.

between the jet and the target surface increases. For the given parameters, the highest Nusselt number was obtained as Nu = 176.08 at H/D = 2, while the lowest Nusselt number was obtained as Nu = 138.85 at H/D = 8. Three different jet types were examined in the experiments: CCJ, CAJ, and SAJ. The effects of all three jets on heat transfer for fixed parameters Re = 6000, A_o = 1.4, and Wo = 67 are compared in Figure 12b. The heat transfer obtained in CCJ, CAJ, and SAJ cases was found to be Nu = 149.08, Nu = 204.55, and Nu = 224, respectively. The lowest heat transfer was obtained for CCJ. It has been

observed that the continuous annular jet significantly increases the heat transfer compared to the circular jet. SAJ, on the other hand, showed a better performance in cooling the target surface compared to CAJ flow.

This study indicated that continuously impinging annular jets on a flat surface provide higher heat transfer than continuously impinging circular jets. This result is also supported by previous study results [11–14]. While continuously impinging circular jets are more effective at the stagnation point, their effect decreases in the wall jet region. It has been determined that continuously impinging annular jets are effective on almost the entire plate surface. It has been understood that synthetic impinging annular jets provide superior performance compared to continuously impinging annular jets. At a constant Reynolds number and a constant jet-target surface distance, the increase in synthetic amplitude caused the effect of the jet to be felt on the entire plate surface. Experimental study results show that the synthetic annular impinging jets can significantly increase heat transfer improvement compared to continuous impinging jets if appropriate parameters are selected.

Uncertainty analysis

In this study, it was determined that the uncertainties occurring during the experiments were caused by measurement errors. Quantities that cause uncertainty arise from measurement errors such as jet velocity, fluid temperature, and surface temperature. For this reason, the method suggested by Holman [40] was used to detect the uncertainties occurring in the experiments.

According to this method, the quantity to be measured in the system is accepted as R and the n independent variables affecting this quantity are x_1, x_2, x_3, ... x_n (Eq.. 18).

$$R = (x_1, x_2, x_3, \ldots\ldots x_n) \tag{18}$$

The measured quantity is expressed as the sum of these variables and the total uncertainty is found with Eq. 19.

$$W_R = \left[\left(\frac{\partial R}{\partial_{x1}} w_1\right)^2 \left(\frac{\partial R}{\partial_{x2}} w_2\right)^2 + \ldots\ldots\ldots + \left(\frac{\partial R}{\partial_{xn}} w_n\right)^2\right]^{1/2} \tag{19}$$

In this study, it is determined that the parameters causing measurement errors are q" heat flux applied to the surface, T_w target surface temperature, T_j temperature of the jet fluid, and U_j main flow velocity measurements. The total uncertainty is calculated by determining the uncertainty of each parameter on the Nusselt number (Eq. 20).

$$W_{Nu} = \left[\left(\frac{\partial Nu}{\partial_q} w_q\right)^2 + \left(\frac{\partial Nu}{\partial_{T_w}} w_{T_w}\right)^2 + \left(\frac{\partial Nu}{\partial_{T_j}} w_{T_j}\right)^2 + \left(\frac{\partial Nu}{\partial_U} w_{U_j}\right)^2\right]^{1/2} \tag{20}$$

According to this method, the average uncertainty of Nusselt numbers was found to be approximately ±4.92 (Eq.. 21).

Table 2. Uncertainties in the devices used in the experiment.

Parameters	Instruments	Accuracy
Data logger	Keithley 2750, (200 data/s)	±0.1%
Velocity	Testo-435 Anemometer, (0.25–20 m/s)	±0.03 m/s
Surface temperature	Omega, K-type (−70°C ... +1000°C)	±0.5°C
Ambient temperature	Omega, K-type (−70°C ... +1000°C)	±0.2°C
Power supply	Ametek Sorensen, XG 6–110 (0-6V), 0-110A	±3W
Frequency	Digital Photo Tachometer (AT-6)	±0.05%

$$\frac{W_{Nu}}{Nu} = \pm 4.92 \tag{21}$$

It can be speculated that this calculated uncertainty rate is at an acceptable level for experiments. The devices used in the study, the features of these devices, and the uncertainties in the parameters are presented in Table 2.

Conclusion

In this study, the cooling of a circular flat surface with constant heat flux (q" = 1200 W/m^2) using a synthetic annular impinging jet was experimentally investigated. In the study, the Reynolds number (6000≤Re ≤ 50000), the distance between the jet and the target surface (2≤H/D ≤ 8), the amplitude of the oscillation (0.47≤A_o ≤1.87) and the oscillation frequency (67≤ Wo ≤ 163) were examined on surface cooling. effects have been investigated. The results are compared with continuously impinging annular jets and continuously impinging annular jet flows.

- It was observed that continuously impinging annular jets provide a lower surface temperature than continuously impinging circular jets, and synthetic impinging annular jets are more effective in surface cooling than continuously impinging annular jets. Continuously impinging annular jets on a flat surface provide higher heat transfer than continuously impinging circular jets.
- Continuously impinging circular jets are more active in the stagnation region and less effective in the wall jet region, while continuously impinging annular jets are less active in the stagnation region and more dominant in the wall jet region. Continuously impinging annular jets are effective on almost the entire plate surface.
- It was determined that surface temperatures decrease significantly as the H/D ratio decreases in all three jet flows. The continuously impinging annular jets provide about 27% higher heat transfer than the continuously impinging circular jets for Re = 50000 and H/D = 2. The heat transfer improved at H/D = 2 by 21% compared to H/D = 8 for Re = 6000, A_o = 1.87 and Wo = 163.
- For Re = 6000, A_o = 1.4, and Wo = 67, the heat transfer obtained in the continuously impinging circular jets, continuously impinging annular jet, and synthetic impinging annular jet was found to be Nu = 149.08, Nu = 204.55, Nu = 224, respectively.
- The experimental study results have shown that the synthetic impinging annular jets can significantly increase heat transfer rate compared to continuously impinging jets if appropriate parameters are selected.

In this study, heat transfer parameters were changed as much as the experimental setup allowed. In future studies, the cooling performance of the surface can be investigated by changing parameters such as target surface geometry, jet geometry, Reynolds number, fluid type, oscillation amplitude, and frequency.

Nomenclature

CAJ	Contunious anular jet
CCJ	Contunious circular jet
SAJ	Syntetic annular jet
A_o	Dimensionless amplitude
B	Dimensionless jet-target surface distance
c_P	Specific heat (kJ/kg^{o}C)
D	Nozzle diameter (m)
h	Heat transfer coefficient (W/m^{2}K)

H	Distance between jet-target surface (m)
k	Conduction coefficient (W/mK)
L	Radius of target plate (m)
N	Total data number
Nu	Nusselt number
Pr	Prandtl number
q"	Heat flux (W/m^2)
Re	Reynolds number
T	Temperature (^oC)
U	Average velocity (m/s)
Wo	Womersley umber
x_m	Piston stroke (m)
Greek symbols	
α	Thermal dissipation coefficient (m^2/s)
μ	Dynamic viscosity (Pa/s)
ν	Kinematic viscosity (m^2/s)
ρ	Density (kg/m^3)
τ	Cycle time
ω	Angular velocity (rad/s)
subscripts	
h	hydraulic
m	mean
in	inner
out	outer
∞	ambient condition
w	wall
j	jet

Acknowledgments

The authors gratefully thank ASU-BAP (Scientific Research Project Unit of Aksaray University, ASU-BAP project no. 2023-05) for the financial support provided.

Disclosure statement

No potential conflict of interest was reported by the author(s).

Funding

The authors gratefully thank ASU-BAP (Scientific Research Project Unit of Aksaray University, ASU-BAP project no. 2023-05) for the financial support provided.

References

[1] H. M. Maghrabie, "Heat transfer intensification of jet impingement using exciting jets, a comprehensive review," *Renewable. Sustainable. Energy. Rev.*, vol. 139, pp. 110684, 2021. DOI: 10.1016/j.rser.2020.110684.

[2] R. Maithani and S. Sharma, "Thermo-hydraulic and exergetic analysis of rectangular channel with integrated jet impingement and roughness," *Exp. Heat. Transfer.*, pp. 1–23, DOI: 10.1080/08916152.2023.2298483. Published online Dec. 30, 2023.

[3] J. Ning, L. Sun, Z. Ren, and X. Gao, "Effect of dry ice jet velocity on cooling characteristics of electronic chip based on optimized geometry," *Exp. Heat Transfer*, pp. 1–19, 2023. DOI: 10.1080/08916152.2023.2232370.

[4] M. V. Philippov, I. A. Chokhar, V. V. Terekhov, V. I. Terekhov, and I. N. Baranov, "Experimental investigation of heat and mass transfer of an annular impinging jet," *J. Phys. Conf. Ser.*, vol. 2039, no. 1, pp. 012028, 2021. DOI: 10.1088/1742-6596/2039/1/012028.

[5] S. D. Barewar, *et al.* "Optimization of jet impingement heat transfer: A review on advanced techniques and parameters," *Therm. Sci. Eng. Prog.*, vol. 39, no. 101697, pp. 101697, 2023. DOI: 10.1016/j.tsep.2023.101697.

[6] P. K. Singh, J. Joshi, and S. K. Sahu, "Thermal characteristics of metal foamed flat plate with circular and elliptical impinging jets," *Exp. Heat. Transfer.*, pp. 1–26, 2023. DOI: 10.1080/08916152.2023.2290268.
[7] L. Dhruw, H. B. Kothadia, and R. A. Kumar, "Area average heat transfer from a vertical flat plate impinged by circular inclined jet," *Exp. Heat. Transfer.*, pp. 1–22, 2023. DOI: 10.1080/08916152.2023.2224787.
[8] R. J. Talapati and V. V. Katti, "Local heat transfer characteristics of circular multiple air jet impinging on a semicircular concave surface," *Exp. Heat. Transfer.*, pp. 1–24, 2023. DOI: 10.1080/08916152.2023.2209894.
[9] R. D. Plant and M. Z. S. Jacob Friedman, "A review of jet impingement cooling," Int. J. Thermofluids., vol. 17, no. 100312, pp. 100312, 2023. DOI: 10.1016/j.ijft.2023.100312.
[10] Y. Zhong, C. Zhou, and Y. Shi, "Effect of the nozzle geometry on flow field and heat transfer in annular jet impingement," *Energies*, vol. 15, no. 4271, pp. 4271, 2022. DOI: 10.3390/en15124271.
[11] S. V. Kalinina, V. I. Terekhov, and K. A. Sharov, "Special features of flow in an annular jet impinging on a barrier," *Fluid. Dyn.*, vol. 50, no. 5, pp. 665–671, 2015. DOI: 10.1134/S0015462815050087.
[12] O. Aydin and B. Markal, "Experimental investigation of coaxial impinging air jets," *Appl. Therm. Eng.*, vol. 141, pp. 1120–1130, 2018. DOI: 10.1016/j.applthermaleng.2018.06.066.
[13] N. Çelik and E. Turgut, "Design analysis of an experimental jet impingement study by using Taguchi method," *Heat. Mass. Transfer.*, vol. 48, no. 8, pp. 1407–1413, 2012. DOI: 10.1007/s00231-012-0989-7.
[14] F. Afroz and M. A. R. Sharif, "Numerical study of turbulent annular impinging jet flow and heat transfer from a flat surface," *Appl. Therm. Eng.*, vol. 138, pp. 154–172, 2018. DOI: 10.1016/j.applthermaleng.2018.04.007.
[15] V. I. Terekhov, S. V. Kalinina, and K. A. Sharov, "Convective heat transfer at annular jet impingement on a flat blockage," *Heat. Mass. Transfer. Phys. Gasdynamics.*, vol. 56, no. 2, pp. 229–234, 2018. DOI: 10.1134/S0018151X18010194.
[16] M. Fenot, E. Dorignac, and R. Lantier, "Heat transfer and flow structure of a hot annular impinging jet," *Inter. J. Therm. Sci.*, vol. 170, no. 107091, pp. 2021, 2021. DOI: 10.1016/j.ijthermalsci.2021.107091.
[17] P. Dutta and H. Chattopadhyay, "Numerical analysis of transport phenomena under turbulent annular impinging jet," *Comput. Thermal. Scien.*, vol. 13, no. 2, pp. 1–19, 2021. DOI: 10.1615/ComputThermalScien.2020035055.
[18] P. Dutta, H. Chattopadhyay, and S. Bhattacharyya, "Numerical investigations on turbulent transport phenomena over a moving surface due to impinging annular jets," *Heat. Transfer. Eng.*, pp. 1–17, 2024. DOI: 10.1080/01457632.2023.2301155.
[19] F. V. Barbosa, S. F. C. F. Teixeira, and J. C. F. Teixeira, "Convection from multiple air jet impingement - a review," *Appl. Therm. Eng.*, vol. 218, no. 119307, pp. 2023, 2023. DOI: 10.1016/j.applthermaleng.2022.119307.
[20] H. Kaya and E. Alp, "Experimental investigation of effect of iron oxide nanofluids with different morphology on heat transfer of multiple impinging jets," *Exp. Heat. Transfer.*, vol. 36, no. 5, pp. 719–733, 2023. DOI: 10.1080/08916152.2023.2212671.
[21] T. Tu, S. Chen, and C. Xu, "Conjugated heat transfer simulation of flow mechanism and heat transfer characteristic of sweeping jet impinging on leading edge in turbine cascade," *Appl. Therm. Eng.*, vol. 236, no. 121839, pp. 121839, 2024. DOI: 10.1016/j.applthermaleng.2023.121839.
[22] B. L. Smith and G. W. Swift, "A comparison between synthetic jets and continuous jets," *Exp. Fluids*, vol. 34, no. 4, pp. 467–472, 2003. DOI: 10.1007/s00348-002-0577-6.
[23] P. Xu, A. S. Mujumdar, H. J. Poh, and B. Yu, "Heat transfer under a pulsed slot turbulent impinging jet at large temperature differences," *Therm. Sci.*, vol. 14, no. 1, pp. 271–281, 2010. DOI: 10.2298/TSCI1001271X.
[24] S. Panda, J. Pasa, and V. Arumuru, "Characterisation of an independently controlled coaxial synthetic jet," *Sens. Actuators. A. Phys.*, vol. 359, no. 114469, pp. 114469, 2023. DOI: 10.1016/j.sna.2023.114469.
[25] O. A. Zargar, R. F. Huang, and C. M. Hsu, "Effect of acoustic excitation on flames of swirling dual-disk double-concentric jets," *Exp. Therm. Fluid Sci.*, vol. 100, pp. 337–348, 2019. DOI: 10.1016/j.expthermflusci.2018.09.018.
[26] J. W. Tan, Y. W. Lyu, J. Z. Zhang, and J. Y. Zhang, "Experimental study on heat transfer enhancement of square-array jet impingement by using an integrated synthetic jet actuator," *Sci. China. Technol. Sci.*, vol. 66, no. 12, pp. 3439–3449, 2023. DOI: 10.1007/s11431-022-2384-6.
[27] Z. Travnicek and V. Tesar, "Annular impinging jet with recirculation zone expanded by acoustic excitation," *Int. J. Heat. Mass. Transfer.*, vol. 47, no. 10–11, pp. 2329–2341, 2004. DOI: 10.1016/j.ijheatmasstransfer.2003.10.032 .
[28] P. Sharma, D. Mirikar, S. K. Sahu, and H. Yadav, "An experimental investigation on the influence of Strouhal number and amplitude on the flow and heat transfer behavior of synthetic jet impingement," *Exp. Heat. Transfer.*, pp. 1–26, 2024. DOI: 10.1080/08916152.2024.2329629.
[29] Z. Trávníček, V. Tesař, Z. Broučková, and K. Peszyński, "Annular impinging jet controlled by radial synthetic jets," *Heat. Transfer. Eng.*, vol. 35, no. 16–17, pp. 1450–1461, 2014. DOI: 10.1080/01457632.2014.889467.
[30] L. D. Mangate and M. B. Chaudhari, "Heat transfer and acoustic study of impinging synthetic jet using diamond and oval shape orifice," *Inter. J. Therm. Sci.*, vol. 89, pp. 100–109, 2015. DOI: 10.1016/j.ijthermalsci.2014.10.006.
[31] T. S. O. Donovan and D. B. Murray, "Heat transfer to an acoustically excited impinging air jet," 5th European Thermal-Sciences Conference, The Netherlands, 2008.
[32] G. Krishan, K. C. Aw, and R. N. Sharma, "Synthetic jet impingement heat transfer enhancement—A review," *Appl. Thermal. Eng.*, vol. 149, pp. 1305–1323, 2019. DOI: 10.1016/j.applthermaleng.2018.12.134.

[33] A. Arshad, M. Jabbal, and Y. Yan, "Synthetic jet actuators for heat transfer enhancement – a critical review," *Int. J. Heat. Mass. Transfer.*, vol. 146, no. 118815, pp. 2020, 2020. DOI: 10.1016/j.ijheatmasstransfer.2019.118815.
[34] X. Tan, J. Zhang, S. Yong, and G. Xie, "An experimental investigation on comparison of synthetic and continuous jets impingement heat transfer," *Int. J. Heat. Mass. Transfer.*, vol. 90, pp. 227–238, 2015. DOI: 10.1016/j.ijheatmasstransfer.2015.06.065.
[35] X. Deng, Z. B. Luo, Z. X. Xia, and W. J. Gong, "Experimental investigation on the flow regime and impingement heat transfer of dual synthetic jet," *Inter. J. Therm. Sci.*, vol. 145, no. 1058642, pp. 105864, 2019. DOI: 10.1016/j.ijthermalsci.2019.02.039.
[36] U. Akdag, S. Akcay, and M. L. Karabayır, "Experimental investigation of the heat transfer characteristics of a pulsating impinging jet on a flat surface," *J. Fac. Eng. Archit. Gaz.*, vol. 38, no. 2, pp. 889–899, 2023. DOI: 10.17341/gazimmfd.1024995.
[37] P. K. Singh, P. K. Upadhyay, H. Yadav, and S. K. Sahu, "An experimental investigation on the thermal behavior of synthetic jets involving non-circular orifices with varying wave patterns," *Exp. Heat. Transfer.*, pp. 1–18, 2023. DOI: 10.1080/08916152.2023.2248475.
[38] P. K. Singh, H. Yadav, P. K. Upadhyay, and S. K. Sahu, "Influence of waveforms on the heat transfer behavior of multi-orifice synthetic jet," *Exp. Heat. Transfer.*, pp. 1–16, 2024. DOI: 10.1080/08916152.2024.2341739.
[39] S. Rakhsha, M. R. Zargarabadi, and S. Saedodin, "Experimental and numerical study of flow and heat transfer from a pulsed jet impinging on a pinned surface," *Exp. Heat Transfer*, vol. 34, no. 4, pp. 376–391, 2021. DOI: 10.1080/08916152.2020.1755388.
[40] J. P. Holman, *Experimental Methods for Engineers*. New York, USA: McGraw-Hill, 2001.